Moisture transport properties of mortar and mortar joint: a NMR study

H.J.P. Brocken*†, O.C.G. Adan† and L. Pel‡

* Department of Architecture and Building Technology,

‡ Department of Physics, Eindhoven, University of Technology, P.O. Box 513, 5600 MB Eindhoven, The Netherlands

† TNO Building and Construction Research, P.O. Box 49, 2600 AA Delft, The Netherlands

The moisture transport in mortar and mortar joint often is an important parameter in degeneration of brick masonry and other block constructions. In this study, the influence of single additives on the moisture transport properties of mortar is investigated. Due to water extraction during brick laying, curing conditions of mortar in mortar joint differ from curing conditions of separately cured mortar. Consequently, the moisture transport properties of mortar joint differ. In addition to the moisture transport in mortar and mortar joint, the moisture transport in brick masonry is investigated. Experimental moisture profiles of water absorption in brick masonry indicate that there is no perfect hydraulic contact at the brick-mortar interfaces.

1 Introduction

In Dutch housing, brick masonry is a common and durable construction material. The durability can be defined as the capability of a material or construction to resist degeneration mechanisms for example as a result of frost and salt attack. Heat and moisture transport play a dominant role in most of these degeneration phenomena. Consequently, a detailed knowledge of the heat and moisture transport is needed for understanding the various degeneration mechanisms involved. The present paper focuses on the moisture transport properties of mortar and mortar joint as studied by Nuclear Magnetic Resonance (NMR). Moisture transport properties are strongly influenced by the curing conditions of mortar. In modern building practice, mortar additives are used to obtain a standardised workability. All these additives influence the moisture transport properties of mortar. Besides in brick masonry, mortar joints are cured in between the bricks. Consequently, water is extracted from the mortar during brick laying, thereby changing curing conditions and moisture transport properties of mortar in mortar joint. Considering the moisture transport in brick masonry, apart from the moisture transport properties of mortar joint and brick, the hydraulic contact between these materials is an important parameter. Especially, the characteristics of this contact strongly determine the moisture transport across the brick-mortar interface.

HERON, Vol. 42, No. 1 (1997) ISSN 0046-7316

2 Theory

The isothermal macroscopic liquid water flux, q_l, in porous material can be described by Darcy's law:

$$q_1 = -K(\theta_1)\nabla\psi(\theta_1) \tag{1}$$

In this equation K [ms^{-1}] is the hydraulic conductivity and ψ [m] the suction, which are both a function of the actual volumetric moisture content θ_l [m^{3}m^{-3}]. Neglecting transport due to the gravity, the outside gas pressure and dissolved salts, the suction is given by:

$$\psi = \frac{1}{g\rho_l}P_{cap}(\theta_1) \tag{2}$$

In this equation $P_{cap}(\theta_l)$ [Nm^{-2}] is the macroscopic capillary pressure, ρ_l [kgm^{-3}] the mass density of liquid water, and g [ms^{-2}] the acceleration of gravity. Liquid water in a non-saturated porous material is now transported because of gradients or inhomogeneities in capillary action only. Under isothermal conditions the capillary pressure and consequently the suction only varies with the moisture content and equation (1) can be rewritten:

$$q_1 = -D_{\theta,1}\nabla\theta_1 \tag{3}$$

where:

$$D_{\theta,1} = K(\theta_1)\left(\frac{\partial\psi(\theta_1)}{\partial\theta_1}\right)_T$$

In this equation $D_{\theta,l}$ [m^{2}s^{-1}] is the isothermal liquid moisture diffusivity.
Combining equation (3) with the conservation of mass and neglecting evaporation, the liquid moisture transport can be described by:

$$\frac{\partial\theta_1}{\partial t} = \frac{\partial}{\partial x}\left(D_{\theta,1}\frac{\partial\theta_1}{\partial x}\right) \tag{4}$$

This diffusion equation was first established by Philip and de Vries [1]. Later Whithaker [2] and Bear [3] gave a more fundamental description.
In the case of two porous materials, e.g., brick and mortar that are bonded to each other, the macroscopic capillary pressure across the material interface should be continuous, hence:

$$\psi_b(\theta_{l,b}) = \psi_m(\theta_{l,m}) \tag{5}$$

In this equation the subscripts 'b' and 'm' indicate the brick and the mortar respectively. Since the suction is a different function of the moisture content for each porous material, condition (5) will result in a jump of the moisture content at the interface of the two materials, hence:

$$\theta_{l,m} = f(\theta_{l,b}) \tag{6}$$

On the other hand, the moisture flux across such a material interface will be continuous:

$$\begin{aligned} q_b &= q_m \\ D_{\theta,b}(\theta_{l,b})\frac{\partial \theta_{l,b}}{\partial x} &= D_{\theta,m}(\theta_{l,m})\frac{\partial \theta_{l,m}}{\partial x} \end{aligned} \tag{7}$$

3 NMR moisture content measurement

The experimental moisture profiles presented in this paper are obtained using nuclear magnetic resonance (NMR). This method offers the possibility to determine moisture content profiles quantitatively, non-destructively and with a high spatial resolution. In a NMR experiment the magnetic moments of the hydrogen nuclei are manipulated by suitably chosen alternating radio frequency fields, resulting in a so called spin-echo signal. The amplitude of the spin-echo signal is proportional to the amount of hydrogen nuclei excited by the radio frequency field. The resonance condition for the nuclei is given by:

$$f = \frac{\gamma}{2\pi} B_0 \tag{8}$$

Here, f is the frequency of the alternating field, γ is the gyromagnetic ratio ($\gamma/2\pi = 42.58$ MHz$/T$ for ^1H) and B_0 is the externally applied static magnetic field. Because of the resonance condition, the method can be made sensitive to hydrogen only and therefore to water.
For the experiments described here, a home built NMR apparatus was used, operating at a frequency of 34 Mhz ($B_0 = 0.8$ T). This apparatus was especially designed to perform quantitative measurements in porous materials with short T_2 relaxation times [4] (unlike standard Magnetic Resonance Imaging (MRI) which is generally used in a qualitative way). A well defined magnetic field gradient was applied, offering a one-dimensional resolution of 1.0 mm. With this NMR apparatus the moisture content at a certain position can be determined within 40 s, with an inaccuracy of 1%.
The experimental set-up for measuring moisture profiles during absorption is given in figure 1. The moisture distribution in a small region (1 to 2 mm) of the sample is measured simultaneously. After determination of the moisture distribution in this small region, the sample is moved vertically over a few mm with the help of a step motor. This is repeated until an entire moisture profile has been measured. Subsequent moisture profiles are measured by repeating the procedure mentioned above. During the measurements a time stamp is added to each point of the experimental moisture profile. An extensive description of the NMR apparatus can be found in [4, 5].

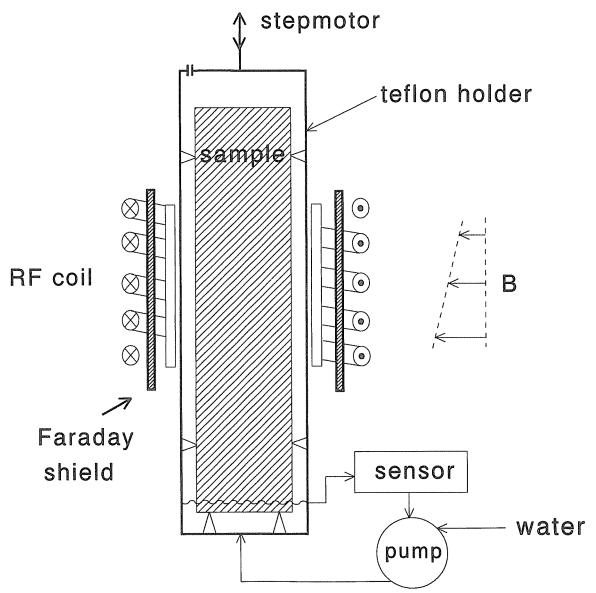

Fig. 1. Experimental probe head for measuring moisture profiles during water absorption.

4 Water absorption and suction of mortar

4.1 *Sample preparation*

To study the influence of additives on the hygric properties of mortar, 5 different mortar types (MA-ME) were investigated. All these mortar types were sand-cement based. Mortar MA contained no additions whereas mortar MB to ME contained single additions of limestone, lime, air entraining agent and water retention agent, respectively. Constituents and characteristics of the various mortar types are summarized in Table 1. In all these mortars a portland cement A (CEM I) was used and the aggregate consisted of a Dutch river sand. The grading characteristics of this (fine) sand mixture fall within the limits of the Dutch Standard 'NEN 3835'. The cement to sand ratio was 1:4.5 (by volume). According to the German Standard 'DIN 1060 Teil 3', the water content of each mortar was set to achieve a defined consistency. To improve the reproducibility of the mortars, the standard mixing procedure of 'DIN 1164 Teil 7' was carried out. The air content of the mortars (after mixing) was determined according to the American Standard 'ASTM C185'. (Note that, as a result of both bleeding of the mortar and evaporation at the top side of the mould, especially in mortar MA, the effective water to cement ratio, wcr_e, was less than the calculated water to cement ratio, wcr_c.)

For the water absorption experiments, cylindrical samples of 20 mm diameter and 50 mm length were cast in cylindrical moulds. These moulds were open at the top side. Additionally, rectangular mortar bars were cast. For suction experiments, cylindrical samples of 45 mm diameter were drilled out of 20 mm slices that were sawn from these bars. Before testing, both the cast samples for the absorption experiments and the mortar bars were cured for at least 28 days at 20°C and 50% RH.

Table 1. The constituents and characteristics of the mortar types MA-ME. The following abbreviations are used: "*scw*" = sand, cement and water, "*aea*" = air entraining agent, "*wra*" = water retention agent (= methyl tylose), "*w/c*" = water/cement and "*a/c*" = additive/cement.

Mortar type	constituents	*w/c* ratio (by mass)	*a/c* ratio (by mass)	aircontent (by volume)
MA	*scw*	1.35	-	5.6
MB	*scw + limestone*	1.15	0.53	4.1
MC	*swc + lime*	1.21	0.27	5.6
MD	*scw + aea*	1.19	$2.9 \cdot 10^{-5}$	13.4
ME	*scw + wra*	1.23	$1.9 \cdot 10^{-3}$	13.2

4.2 *Water absorption*

The moisture profiles during water absorption were measured using the NMR apparatus as described in section 3. In case of water absorption, the measured profiles can be related by the Boltzmann transformation, $\lambda = xt^{-1/2}$ [6,7]. In figure 2, Boltzmann transformations are plotted for mortar MA to ME. For mortar MB to ME these transformations yield a distinct curve on which the data of various profiles coincide (see Fig. 2a). This indicates that the moisture diffusivity does not depend on the position in the sample and thereby that the sample is homogeneous with respect to the moisture transport. The moisture transport therefore can be modeled by a diffusion equation.

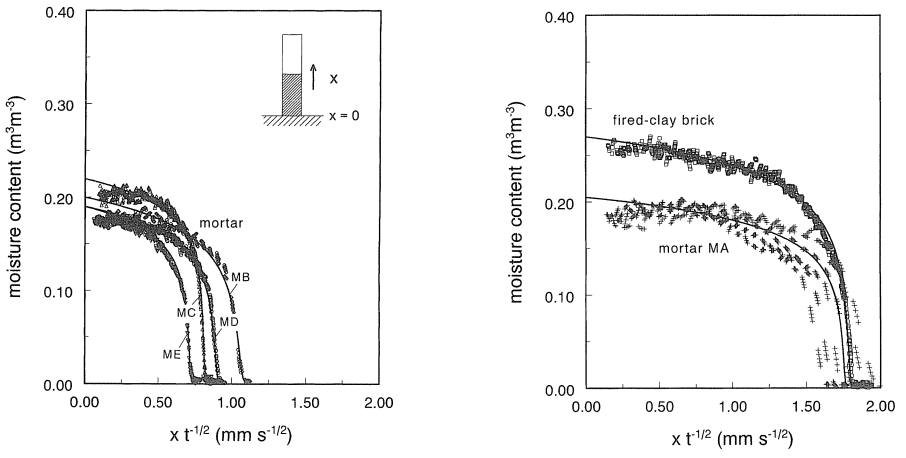

(a) *(b)*

Fig. 2. Boltzmann transformation of the measured moisture profiles (a) for mortar MB (◇), MC (△), MD (○) and ME (▽), and (b) for mortar MA (+) and fired-clay brick (□). (——) Boltzmann transformation of the simulated moisture profiles based on an exponential moisture diffusivity. The inset in Fig. 2a shows the experimental set-up.

On the contrary, in case of mortar MA, Boltzmann transformation does not yield a distinct curve of coinciding profiles (see Fig. 2b). Obviously, mortar samples of mortar MA are inhomogeneous so that the moisture diffusivity depends on the position and the Boltzmann transformation can not be applied.
Often an exponential relation for the liquid moisture diffusivity is assumed [5, 6]:

$$D_{\theta,1}(\theta_1) = D_{\theta,0}\exp(\beta\theta_{cap}) \tag{9}$$

Based on this exponential relation, the parameters $D_{\theta,0}$ and β were fitted by computer simulations of the absorption. Using the experimental moisture diffusivity, the water absorption profiles were calculated. The Boltzmann transformations of the calculated moisture profiles are added in Figs. 2, showing a satisfactory agreement with the experimental observations. From the experimental moisture diffusivity the sorptivity, S, and the initial rate of absorption, IRA, for initial dry materials can be calculated. The results are given in Table 2, together with the averaged capillary moisture content, θ_{cap}. The results show that the sorptivity of mortar tends to decrease by respectively adding limestone, lime, air entraining agent and water retention agent to the mortar. Each of these additives binds water and, while curing of the mortar samples, may therefore give a better water distribution. Moreover, in that case the compaction of these mortars will have been slower and consequently the microstructure becomes more dense, resulting in a decrease of the sorptivity.
The sorptivity of mortar MA appears to be higher than that of other mortars. However, due to the inhomogeneity of mortar MA, this result should be considered with some reservation. Mortar MB, MC and MD are in the same range.

Table 2. The capillary moisture content, θ_{cap}, and the sorptivity, S, and the initial rate of absorption, IRA, for initial dry materials determined using the experimental moisture diffusivity. The sorptivity is given both in case the mortars are cured for 28 days in moulds and thereafter for 7 weeks under water. (* number of samples; Note that the values presented in this table are averages of only 2 to 4 samples)

Material	θ_{cap} [m^3m^{-3}]	S-28 days [kg $m^{-2}s^{-0.5}$]	IRA [kg $m^{-2}min^{-1}$]	S-7 weeks [kg $m^{-2}s^{-0.5}$]
[2)*] mortart MA	0.20	0.29	2.2	0.22
[2)] mortart MB	0.20	0.19	1.4	0.15
[2)] mortart MC	0.22	0.16	1.2	0.13
[2)] mortart MD	0.19	0.17	1.3	0.15
[2)] mortart ME	0.19	0.12	1.0	0.12
[4)] fired-clay brick	0.27	0.42	3.3	-

To check the inhomogeneity of mortar samples, (atmospheric) capillary moisture content profiles were measured. Two typical profiles for mortar MA and MD are plotted in figure 3, showing that the capillary moisture content is not evenly distributed in the sample. Since the samples were not covered during preparation, the inhomogeneity in the mortar samples might be caused by evaporation at the open top side of the mould. This introduces deviations in hydration conditions of the cement particles as a function of position in the sample. Furthermore, as a result of bleeding the water to cement ratio will also be a function of position. This bleeding was especially observed in case of mortar MA. The moisture profiles presented in Fig. 2 were measured in case of absorption from the top side of the samples. From this topside, the capillary moisture content increases. For mortar MA the highest capillary moisture content is found at 15 mm from the top whereas for mortar MD the highest value is found at 25 mm from the top. Considering the top 40 mm of the samples, for mortar MD the lowest value deviates by approximately 0.02 m^3m^{-3} from the highest value whereas for mortar MA this deviation is approximately twice as much. The inhomogeneity of the other mortars was about the same as for mortar MD.

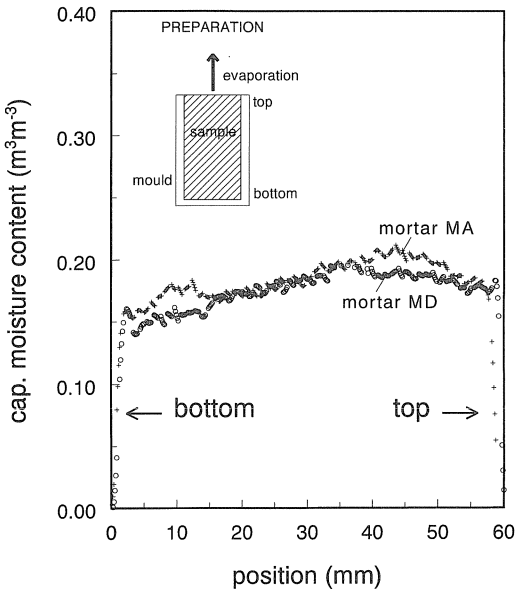

Fig. 3. Profile of the capillary moisture content as a function of position in a sample of mortar MA (+) and MD ( ), cast in a mould.

In order to test whether additional curing of cement particles in the mortar has effect on the absorption, experiments were performed after keeping samples under water for a period of 7 weeks. The samples were dried before actually testing the water absorption. The resulting sorptivities are added in Table 2. In case of mortar MA, the sorptivity apparently decreased. For mortar MB to MD the decrease of the sorptivity was less distinct, whereas in case of mortar ME the sorptivity practically remained the same. Therefore only in case of mortar MA, the pore distribution apparently changed by putting the samples under water.

4.3 *Suction*

The experimental determination of the suction curves or capillary pressure curves is carried out according to the set-up presented in the inset of figure 4. An initially saturated sample is placed on a semi-permeable membrane sealing an air-tight chamber. This membrane is permeable to water only. The curves are measured point by point by applying a certain air pressure (up to 12 bar) on the samples and waiting until an equilibrium moisture content is reached: for each point on the curve this takes about 6 to 8 days. The curves given in Fig. 4 therefore represent an equilibrium situation where no moisture transport occurs. Consequently, the air pressure will be equal to the macroscopic capillary pressure.

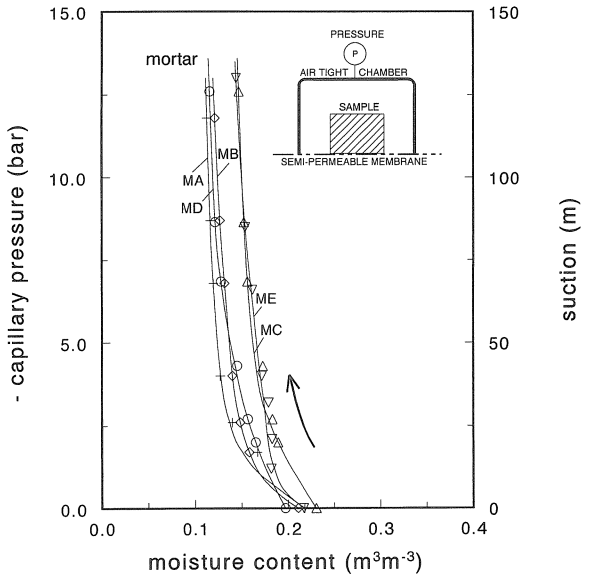

Fig. 4. Capillary pressure curve of mortar MA (+), MB (◇), MC (△), MD (□) *and* ME (▽). *Only the drying curves for capillary saturated samples are measured. The inset shows the set-up of the experiment.*

In Fig. 4 the measured suction curves for mortar MA to ME are plotted. At a pressure of approximately 12 bar, still not all water is pressed out of the samples. This indicates that the water is in cylindrical pores smaller then 10^{-7} m. (Note that the water may also be in some pores that are not connected directly to the membrane. In this case the measured points in Fig. 4 do not represent the equilibrium moisture content.) The curves of mortar MA, MB and MD more or less coincide and so do the curves for mortar MC and ME, although they are shifted to somewhat higher moisture contents. In case of mortar ME this observation corresponds with the absorption experiments: mortar ME has more small pores and, hence, a higher suction and a lower absorption rate or sorptivity.

5 Water absorption and suction of brick

The characteristics of mortar studied in the previous section will deviate from those of actual mortar joints in brick masonry. During brick laying, water is extracted from the mortar. This water extraction is related to the water retentivity of the mortar and both to the water absorption rate and the suction of the brick. Besides these parameters of the brick are needed to study the water absorption in cured brick masonry.

For fired-clay brick the Boltzmann transformation of measured water absorption profiles yields a distinct curve on which the data coincide (see Fig. 2b). The solid curve in Fig. 2b denotes results of simulations based on an exponential relation (eq. 9) as with the mortar (see section 4). The computer simulation also gives a satisfactory description of the observed moisture profiles. The sorptivity, S, and the initial rate of absorption, IRA, for initial dry fired-clay brick both determined using the experimental moisture diffusivity and the capillary moisture content, θ_{cap}, are given in Table 2. Obviously the water absorption rate or sorptivity of fired-clay brick is higher than that of mortar. Fig. 5 gives the measured suction curve of fired-clay brick. The capillary moisture content of fired-clay brick is higher as compared with that of mortar (see Fig. 4). However the suction curves of the various mortar types (see Fig. 4) increase more rapidly for decreasing moisture contents than the suction curve of fired-clay brick. This indicates that the mortars mainly contain small pores whereas fired-clay brick also contains a reasonable amount of larger pores (> 10^{-6} m). The difference in absorption characteristics of fired-clay brick and mortar agrees with the suction curves; in mortar mainly small pores contribute to the water absorption, and hence mortar has a lower absorption rate than fired-clay brick.

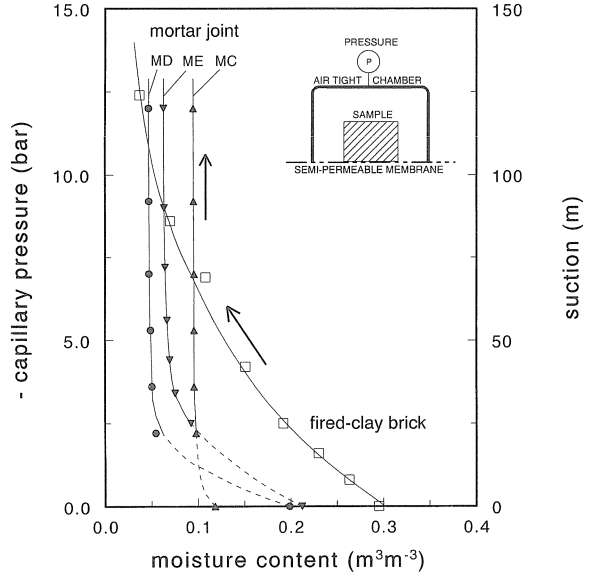

Fig. 5. Capillary pressure curve of fired-clay brick ( ) and mortar joint MC (▲), MD (●) *and* ME (▼). *Only the drying curves for capillary saturated samples are measured. The inset shows the set-up of the experiment.*

6 Water extraction from mortar

As a result of water extraction from mortar during brick laying, the water to cement ratio of mortar in mortar joints is less than the water to cement ratio of mortar samples as investigated in section 4. Apart from the additives used in the mortar, the curing conditions and the actual performance of mortar joint strongly depend on this water extraction. In this section, this phenomenon is briefly described. A more extensive description can be found in [8].

The mortar samples as used in section 4 all consist of water, cement and a single additive. However in modern building practice, a mix of various additives is commonly applied, in order to adjust workability of the mortar for specific application. In case of water extraction experiments, the cement and the additives used in the mortar, slightly differ from those as used for the mortar samples of section 4. A detailed description of these constituents and ratios is given in [8]. In the set-up of the water extraction experiments, a cylindrical brick sample of 20 mm diameter and 50 mm length was placed upon a 6 mm thick layer of fresh mortar. This 6 mm corresponds with half of the common thickness of mortar joints used in Dutch building practice. Immediately after the brick was placed upon the mortar and water transport from mortar to brick starts, corresponding moisture profiles were measured each 90 seconds. The profiles in the mortar remained rather flat during the water extraction process [8]. Therefore a local moisture content somewhere in the mortar layer represents the average moisture content of the entire mortar layer. Figure 6 gives an example of the measured average moisture content as a function of time. Most of the water is extracted from the

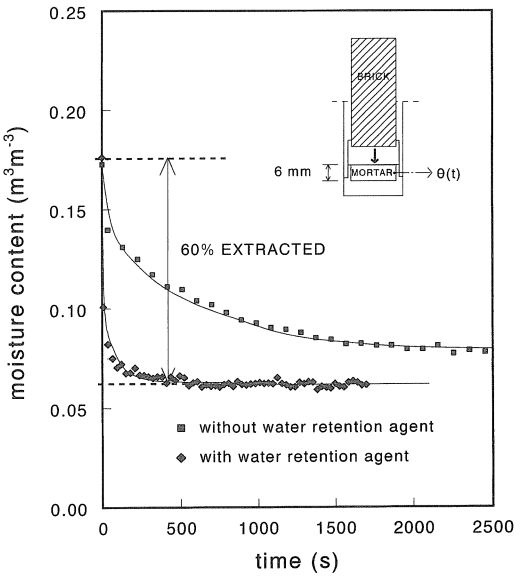

Fig. 6. Local moisture content in the mortar as a function of time, during water extraction by a fired-clay brick. The moisture contents are plotted in the case of initially dry fired-clay bricks (I_{RA} = 3.3 kg m^{-2}min^{-1}) for mortar (■) with and (◆) without water retention agent added to it. (——) Guide to the eye.

mortar within the first 90 seconds. Prewetting the bricks up to 50% of the capillary moisture content neither did affect the water extraction rate, nor the amount of water that is extracted [8]. Addition of water retention agent to the mortar apparently slows down the water extraction. In this case the final moisture content of the mortar is somewhat higher than the final moisture content of the mortar without water retention agent; in our experiments, after 2 hours, this moisture content was about 10% higher.
In case of the tested fired-clay brick, approximately 60% of the water is extracted from the various mortars as used in the experiments. Consequently, the actual water to cement ratio of mortar joint is substantially lower than the initial water to cement ratios of the mortars cured separately as in case of the samples used in section 4. Deviations in moisture transport properties of actual mortar joints in brick masonry and separately cured mortar samples therefore are to be expected and the effect of single additives on the sorptivity of separately cured mortar should be considered indicative only.

7 Suction of mortar joint

As indicated in the previous section, the curing conditions for mortar joint in masonry will differ from those for separately cured mortar samples. Therefore mortar joint samples of 12 mm thickness were fabricated by brick laying. To facilitate this, a special filter paper [9] was placed between mortar and brick so mortar joint slices and bricks could be separated easily after curing. The same mortar types as in section 4 were used. For the suction experiments, cylindrical bars of 45 mm diameter were drilled out of the mortar joint slices. However, due to experimental limitations, the water absorption could not be measured for these samples of 12 mm thickness.
The measured suction curves for mortar joint MC, MD and ME are included in Fig. 5. During preparation (sawing & drilling) all fabricated mortar joint slices of mortar MA and MB were completely cracked. Therefore the suction curves for these mortars have not been measured up to now. The curves that are drawn through the measured points are only given as a guide to the eye. Especially at low capillary pressures, due to the limited number of experimental points, there is only minor experimental evidence that in this range, the course of these curves is correct. The capillary moisture content (i.e. the porosity) of mortar joint MC is less than that of mortar joint MD and ME. Comparing the suction curves of the various mortar joints, for a small increase of the capillary pressure, for mortar joint MD and ME clearly more water is pressed out than for mortar joint MC. This indicates that for mortar joint MD and ME, mainly larger pores contribute to this high porosity. Comparing the curves of various mortar joints cured in between bricks and the corresponding mortars cured separately (Fig. 4 and Fig. 5), the capillary moisture content or porosity of mortar joint MC is smaller than that of separately cured mortar. The porosity of mortar joint MD and ME, however, nearly remained unaltered. Compared to the curves in Fig. 4, for all mortar joints more water is pressed out at the same capillary pressures, indicating that less small pores occur in these mortar joints.

8 Moisture transport over brick-mortar interface

To investigate the water absorption across brick-mortar interfaces, small masonry segments of four initial dry fired-clay bricks with 12 mm mortar joints (types MA-ME) were fabricated. Before the actual brick laying, brick surfaces were smoothed, i.e., the sanded sides were sliced off, to improve reproducibility. The masonry segments were cured for one day under damp cloths and thereafter for a period of 28 days at 20°C and 50% RH. Cylindrical bars of 20 mm diameter were drilled out of these segments in a direction normal to the mortar joints. This section mainly focuses on the experimental results of masonry samples of fired-clay brick and mortar joint MD. Other mortar types showed similar results.

The measured moisture profiles during water absorption in a masonry sample of fired-clay brick and mortar joint MD, are plotted in figure 7a and 7b. The figures show that the water absorption front quickly reaches the first brick-mortar interface. Next, moisture profiles develop in the first mortar joint. Since mortar joint absorbs water rather slowly, the first brick quickly gets saturated. When the front reaches the next mortar-brick interface, the water is slowly absorbed by the second brick. Obviously the absorption rate in this brick is reduced, governed by the permeability of the mortar joint. At the second mortar joint, almost no moisture transport occurs across the brick-mortar interface. As a result a flat profile develops in the second brick and the moisture content in this brick starts to increase until saturation. The entire process took about 4 days in this experiment. Figure 7b reveals that the second mortar joint hardly absorbs any water, even at full saturation of the second brick.

A numerical simulation of the water absorption in brick masonry, performed using routines from the NAG-library [10], is plotted in figure 8. In this simulation the moisture diffusivity as determined for fired-clay brick (section 5) and mortar MD (section 4) are used. Corresponding suctions at the interfaces of both materials (eq. 5) are deduced from the experimental suction curves of fired-clay brick (section 5) and mortar joint MD (section 7). Fig. 8 shows that the water absorption as calculated is much faster compared to the actual water absorption as measured (Fig. 7). This might be caused by the moisture diffusivity of *mortar* which is used in the calculation; most probably the actual moisture diffusivity of *mortar joint* is less. However lowering this parameter to 20% of its initial value, does not sufficiently slow down the water absorption. On the contrary, the decrease of the water absorption rate was negligible, indicating that there is an additional hydraulic contact resistance at the interface of the materials. At this moment further research therefore is focused on the characteristics of moisture transport across these brick-mortar interfaces.

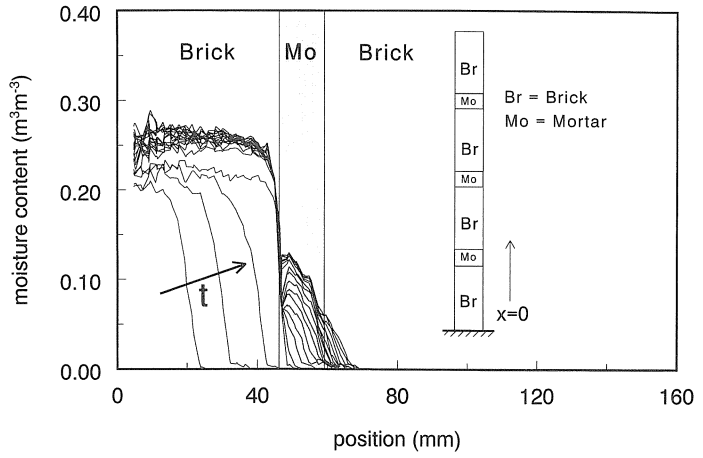

7a.

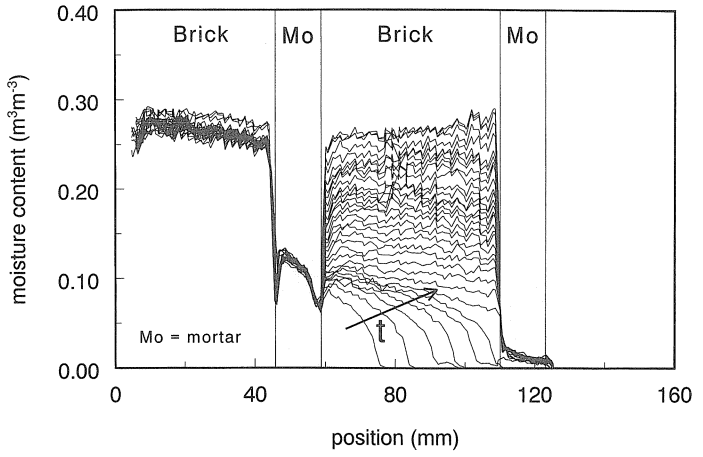

7b.

Fig. 7. Moisture profiles measured during the water absorption in a brick masonry segment of fired-clay brick and mortar joint MD. *The first 20 profiles were measured (a) continuously during the first 2 hours of absorption whereas the next profiles were measured (b) at time intervals of 2 hours. The experiment lasted 4 days. Shaded areas correspond with the mortar joints. The inset in Fig. 7a shows the experimental set-up.*

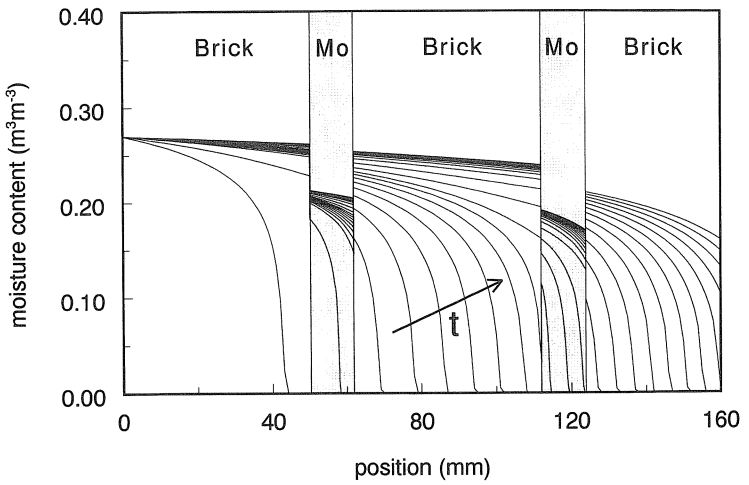

Fig. 8. *Simulated moisture profiles at subsequent time intervals of 5 minutes, assuming perfect hydraulic contact. In total 120 minutes are simulated. The shaded areas indicate the mortar layers.*

9. Conclusions

Water absorption experiments were performed to test the influence of single additives on the moisture transport properties of mortar. The results of these experiments show that the sorptivity of mortar decreases by respectively adding limestone, lime, air entraining agent and water retention agent to the mortar. Due to water extraction from mortar during brick laying the curing conditions of mortar joint differ from those for separately cured mortar; i.e., the water to cement ratios of mortar in actual mortar joints are less than the water to cement ratios of separately cured mortar samples. As a result the suction curves change. For mortar joint, the suction curves indicate that less small pores are present. For mortars with single additions of air entraining agent or water retention agent (mortar MD and ME), the porosity of mortar in a mortar joint is more or less equal. The suction curves for these mortar joints therefore suggest that mainly larger pores contribute to this high porosity.

Water absorption experiments with masonry samples, indicate that the hydraulic contact between successive layers of fired-clay brick and mortar joint is not perfect. This suggests that there is a hydraulic contact resistance at the interfaces. Further research is therefore focused on this contact phenomenon.

Acknowledgements

The authors wish to acknowledge the indispensable experimental help of H.R. Smolders of the Department of Architecture and Building Technology of the Eindhoven University of Technology and M.E. Spiekman of the Department of Civil Engineering of the Delft University of Technology. We also wish to thank H. Smulders and A.W.B. Theuws of the EUT for their help in preparing the samples and modifying several experimental set-ups.

References

1. PHILIP, J.R. and VRIES, D.A. de, Moisture movement in porous materials under temperature gradients, *Trans. Am. Geophys. Un.* **38**, 222-232 (1957).
2. WHITAKER, S., Simultaneous heat, mass and momentum transfer in porous media: A theory of drying porous media, *Adv. Heat transfer* **13**, 119-200 (1977).
3. BEAR, J. and BACHMAT, Y., Introduction to modeling of transport phenomena in porous media, Vol. 4, Kluwer, Dordrecht, the Netherlands (1990).
4. KOPINGA, K. and PEL, L., One-dimensional scanning of moisture in porous materials with NMR, *Rev. Sci. Instrum.* **65**, 3673-3681 (1994).
5. PEL, L., Moisture transport in porous building materials, Ph. D. thesis, Eindhoven University of Technology, the Netherlands (1995).
6. PEL, L., KOPINGA, K., BERTRAM, G. and LANG, G., Water absorption in fired-clay brick observed by NMR scanning, *J. Phys. D: Appl. Phys.* **28**, 675-680 (1995).
7. GARDNER, W.R. and MAYHUGH, M.S., Solutions and tests of the diffusion equation for the movement of water in soil, *Soil. Sci. Soc. Am. Proc.* **22**, 197-201 (1958).
8. BROCKEN, H.J.P., SPIEKMAN M.E., PEL L., KOPINGA, K. and LARBI, J.A., Water extraction out of mortar during brick laying: A NMR study, *accepted for publication in Materials and Structures* (1996).
9. Vörlaufige Richtlinie zur Ergänzung der Eignungsprüfung von Mauermörtel, Mauerwerksbau aktuell DGfM e.V. (1992).
10. The NAG Numerical Fortran Library, Mark 16, NAG, Oxford (1991).